

## Orientational field dependence of low-lying excitations in the mixed state of unconventional superconductors

P. Miranović, N. Nakai, M. Ichioka, and K. Machida

*Department of Physics, Okayama University, Okayama 700-8530, Japan*

(Received 16 May 2003; published 6 August 2003)

Orientational field dependence of the zero-energy density of states (ZEDOS) is calculated for superconductors with the polar state (line node), axial state (point node), and three-dimensional  $d$ -wave state. Depending on the gap topology and the relative field direction the field dependencies of ZEDOS sensitively differ, providing us a useful and practical method to identify the gap topology. It is also demonstrated that for  $d$ -wave state the field rotation in the basal plane shows a sizable oscillation ( $\sim 3\%$ ) of ZEDOS. This is directly measurable in low- $T$  specific heat experiment in the mixed state.

DOI: 10.1103/PhysRevB.68.052501

PACS number(s): 74.25.Bt, 74.25.Op

Much attention has been focused on various unconventional superconductors, ranging from high- $T_c$  cuprates, heavy Fermion materials, Boro-carbides,  $\text{MgB}_2$ , to Skutterudite  $\text{PrOs}_4\text{Sb}_{12}$ . The unconventionality is associated with the gap anisotropy of the orbital function in addition to the spin structure of the Cooper pair. It is quite important to determine the detailed nodal topology of the gap function; either point or line node and their location on the Fermi surface. The determination of these characteristics is expected to lead to an understanding to the pairing mechanism of exotic superconductors.<sup>1</sup>

There are several experimental methods to probe the gap anisotropy. One can basically distinguish the line and point nodes because these give rise to different and distinct power law temperature ( $T$ ) dependence in various physical quantities. As for the orientation of these nodes, there are only a few ways to probe it. The field-dependent thermal conductivity  $\kappa(H)$  and the polarization-dependent sound attenuation are typical ones. By measuring  $\kappa(H, \alpha)$  for different field direction  $\alpha$  one can detect the location of the node in principle because the nodal quasiparticles (QP) under  $H$  with zero-energy transport heat current. In fact, a series of experiments by Izawa *et al.*<sup>2</sup> have determined the location of nodes in several systems. These transport measurements are, however, inevitably involved by the scattering time effect and localization effect of nodal QP, which hamper the determination of the nodal direction in some cases.<sup>3</sup>

Here we propose another method based on thermodynamics: The Sommerfeld coefficient  $\gamma$  of the  $T$ -linear specific heat at lower  $T$  is most fundamental physical quantity in Fermionic systems of interest. Since the nodal QP created around a vortex core in the mixed state sensitively reflect its gap structure, the angle-dependent  $\gamma(H, \alpha)$  can yield characteristic oscillation pattern relative to the nodal position under a fixed  $H$ . Recent angle-resolved  $\gamma(H, \alpha)$  measurement on  $\text{YNi}_2\text{B}_2\text{C}$  by Park *et al.*<sup>4</sup> demonstrates a fourfold oscillation in the basal plane whose amplitude  $\sim 4\%$ , nicely coinciding with  $\kappa(H, \alpha)$  experiment by Izawa *et al.*<sup>2</sup> They agree with the nodal direction [100], but disagree with the topology [point (line) in the latter (former)]. The observed oscillation amplitude ( $\sim 4\%$ ) in  $\gamma(H, \alpha)$  is far off the theoretical prediction ( $\sim 30\%$ ) based on the so-called Doppler shift

argument,<sup>12</sup> which is qualitative in nature (see discussion in Ref. 5). In this paper we calculate the zero-energy density of states (ZEDOS) in the mixed state for various situations—its direction dependence for the polar and axial state and the angular dependence for  $d$ -wave state, in order to examine the experimental feasibility. We develop a full three-dimensional (3D) computation based on quasiclassical framework, which is valid for superconductors with  $k_F \xi \gg 1$  ( $k_F$  Fermi wave number and  $\xi$  the coherence length). This kind of calculation gives quantitatively reliable results. Spherical Fermi surface has been used in our calculation to enlighten the role of gap nodes in low-energy excitations.

Anisotropic pairing is routinely analyzed within the separable model of pairing potential  $V(\mathbf{k}, \mathbf{k}') = V_0 \Omega(\mathbf{k}) \Omega(\mathbf{k}')$ . Then order parameter takes the following form:  $\Delta(\mathbf{r}, \mathbf{k}) = \Psi(\mathbf{r}) \Omega(\mathbf{k})$ . In the clean limit, quasiclassical equations read as

$$\left[ 2\hbar\omega_n + \hbar\mathbf{v} \left( \nabla + \frac{2\pi i}{\Phi_0} \mathbf{A} \right) \right] f = 2\Psi(\mathbf{r}) \Omega(\phi, \theta) g, \quad (1)$$

$$\left[ 2\hbar\omega_n - \hbar\mathbf{v} \left( \nabla - \frac{2\pi i}{\Phi_0} \mathbf{A} \right) \right] f^\dagger = 2\Psi^*(\mathbf{r}) \Omega(\phi, \theta) g. \quad (2)$$

Here  $\hbar\omega_n = \pi T(2n+1)$  with integer  $n$  are Matsubara frequencies,  $\mathbf{v}$  is Fermi velocity,  $\Phi_0$  is flux quantum, and  $f, f^\dagger, g$  are Green's functions integrated over energy normalized so that  $ff^\dagger + g^2 = 1$ . The Fermi surface is assumed to be sphere. Order parameter  $\Psi(\mathbf{r})$  and vector potential  $\mathbf{A}(\mathbf{r})$  are obtained selfconsistently from the following equations:

$$\Psi(\mathbf{r}) \ln \frac{T_c}{T} = 2\pi T \sum_{\omega_n > 0} \left[ \frac{\Psi(\mathbf{r})}{\hbar\omega_n} - \langle \Omega(\phi, \theta) f \rangle \right], \quad (3)$$

$$\nabla \times \nabla \times \mathbf{A}(\mathbf{r}) = - \frac{4\pi^2 \hbar N_0 T}{\Phi_0} \text{Im} \sum_{\omega_n > 0} \langle g \mathbf{v} \rangle. \quad (4)$$

Average over the Fermi surface is denoted as  $\langle \dots \rangle$ . First, polar state with a line node  $\Omega(\phi, \theta) = \sqrt{3} \cos \theta$  and axial state with point nodes  $\Omega(\phi, \theta) = \sqrt{3/2} \sin \theta$  are analyzed. Polar and azimuthal angle refer to the coordinate system with  $z$  axis that coincide with  $c$  crystal direction. Factors  $\sqrt{3}$  and

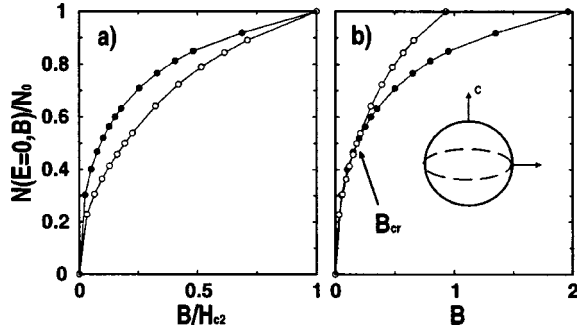


FIG. 1. (a) Field dependence of ZEDOS for polar state. Scaling factor  $H_{c2}$  is different for each direction. The best fit to low-field ( $B < 0.25H_{c2}$ ) dependence is  $N(E=0, B)/N_0 = \gamma(B)/\gamma_N \approx 1.14 \times (B/H_{c2})^{0.35}$  for  $H\parallel c$  (full circles) and  $1.06 \times (B/H_{c2})^{0.45}$  for  $H\perp c$  (empty circles). (b) ZEDOS against induction  $B$  (in dimensionless units).

$\sqrt{3/2}$  assure that average of  $|\Omega(\phi, \theta)|^2$  over the spherical Fermi surface is unity. We are interested in Green's function  $g(\mathbf{r}, \mathbf{v}, \omega)$  that describe QP excitations associated with vortices. The QP density of states  $N(E)$  with energy  $E$  relative to the Fermi level is defined as

$$\frac{N(E)}{N_0} = \frac{\langle N(E, \mathbf{v}) \rangle}{N_0} = \langle \text{Re } g(\mathbf{r}, \mathbf{v}, \omega \rightarrow 0^+ - iE) \rangle, \quad (5)$$

where  $N_0$  is ZEDOS in the normal state. Green's function  $g(\mathbf{r})$  spatially averaged over vortex lattice unit cell is denoted as  $\bar{g}(\mathbf{r})$ . We focus on ZEDOS at low temperatures. This is because low temperature specific heat is  $C_s = \gamma(B)T = 2\pi^2\hbar^2 N(E=0, B)T/3$ . Therefore, the equations are solved for  $T=0.1T_c$ . It is sufficient to know Green's function only in the vortex lattice unit cell, which is divided in mesh  $41 \times 41$ . Once the order parameter and vector potential are obtained selfconsistently, Eqs. (1) and (2) are solved again for  $\omega \rightarrow 0^+$ . Typically, we choose  $\omega = 0.001\pi T_c/\hbar$ . Method of solution is extended from Ref. 6 and details will be described elsewhere.<sup>7</sup> Here we present the results.

In Fig. 1 field dependence of ZEDOS for polar state with a line node is shown for  $H\parallel c$  (full circles) and  $H\perp c$  (empty circles). Ratio  $N(E=0, B)/N_0$  at low  $T$  is equal to  $\gamma(B)/\gamma_N$ , where  $\gamma(B)T$  ( $\gamma_N T$ ) is low  $T$  specific heat of superconducting (normal) phase. We discuss the power-law exponent of  $B$  dependence of ZEDOS. It is difficult to fit the data with a single power-law function  $(B/H_{c2})^\beta$ . At least in low field we can estimate  $N(E=0, B)/N_0 \sim (B/H_{c2})^{0.35}$  for  $H\parallel c$ , i.e., very steep increase with field. Here is the explanation. The most important contribution to ZEDOS is coming from QP that flow in the plane perpendicular to the applied field. For  $H\parallel c$  geometry, those QP experience zero-energy gap. They are easily excited and extended outside of the vortex core even in low field in comparison to  $s$ -wave superconductors. The outcome is steep increase of ZEDOS with field. Experimentally similar small exponent is observed in  $\text{MgB}_2$ . The physics is analogous to the case of polar state. Small exponent is coming from the small gap at the  $\pi$  band<sup>8</sup> in  $\text{MgB}_2$ , while coming from the line node in the polar state. For perpendicular orientation  $H\perp c$  (empty circles) the problem is analogous

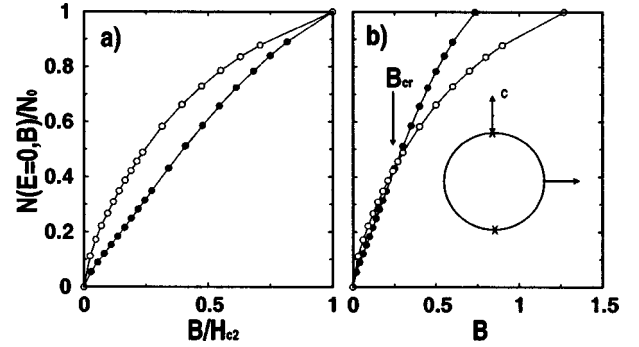


FIG. 2. (a) Field dependence of ZEDOS for axial state. Scaling factor  $H_{c2}$  is different for each direction. The best fit to low-field ( $B < 0.25H_{c2}$ ) dependence is  $N(E=0, B)/N_0 = \gamma(B)/\gamma_N \approx 1.25 \times (B/H_{c2})^{0.64}$  for  $H\perp c$  (empty circles). (b) ZEDOS against induction  $B$  (in dimensionless units).

to that of 2D  $d$ -wave case for fields along the  $c$ -axis. Power law with exponent  $\beta \approx 0.45$  calculated here should be compared with self-consistent calculation on cylindrical Fermi surface and 2D  $d$ -wave gap function, which reveals  $N(E=0, B)/N_0 \sim (B/H_{c2})^{0.43}$  power law.<sup>6</sup> For this geometry  $H\perp c$ , QP in plane  $\perp H$  experience zero gap only if their momentum is in basal plane. Therefore, they are more difficult to excite compared to parallel geometry  $H\parallel c$ , hence the exponent  $\beta$  is bigger.

It is important to emphasize that ZEDOS in Fig. 1(a) is plotted against  $B/H_{c2}$ , where  $H_{c2}$  is different for each geometry. For polar state, there is a large anisotropy of upper critical field  $H_{c2}^{\parallel c} \approx 2H_{c2}^{\perp c}$ . When plotted versus magnetic field, Fig. 1(b), ZEDOS lines crosses at some critical field  $B_{cr}$ . Therefore, by rotating magnetic field from  $c$  axis toward the basal plane, ZEDOS may increase or decrease depending on field value.

For axial state with two point nodes and  $H\parallel c$ , energy gap is small only for small fraction of QP that flow along the  $c$  axis, which makes small contribution to total ZEDOS. In this geometry, ZEDOS resembles that in  $s$ -wave superconductors. Most of the low-energy QP are trapped at vortex cores, at least in low field, thus  $N(E=0, B)/N_0 \sim B/H_{c2}$ . This is confirmed by numerical calculation shown in Fig. 2(a) (full circles). For field  $H\perp c$  (empty circles) power-law exponent is smaller than that in line node polar state for both field geometries, Fig. 1(a). Roughly speaking, the larger is the angular area of suppressed gap, the faster ZEDOS is increasing with induction  $B$ . Note that the field dependence  $N(E=0, B)/N_0 \sim (B/H_{c2}) \ln(B/H_{c2})$  predicted by the Doppler shift calculation for point node case<sup>9</sup> is far off the present result in Fig. 2, warning us the range of its applicability. Similar to the polar state, ZEDOS curves for two field directions cross at some critical field  $B_{cr}$ , as shown in Fig. 2(b). Assuming that the role of the anisotropic Fermi surface is merely to shift the  $H_{c2}$  values, data in Figs. 1(a) and 2(a) may be viewed as independent of the ratio  $H_{c2}^{\parallel c}/H_{c2}^{\perp c}$ .

We show the importance of the mutual arrangement of line node and magnetic field on ZEDOS. In this sense it is interesting to examine 3D version of  $k_x^2 - k_y^2$  symmetry of the gap function, which is given by  $\Omega(\phi, \theta)$

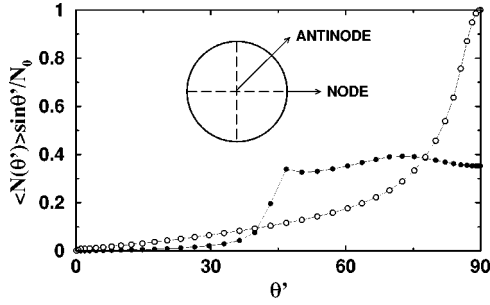


FIG. 3. Angle-resolved ZEDOS averaged over angle  $\phi'$  in plane perpendicular to field,  $\langle N(\theta') \rangle / N_0 = (1/2\pi) \int N(E=0, \mathbf{v}) d\phi'$  for antinode (full circles) and node (empty circles) field directions. Line node is schematically presented with dashed line in the inset. Magnetic induction  $B = 0.0217 H_{c2}^{node}$  ( $H_{c2}^{node}/H_{c2}^{antinode} = 0.828$  at  $T = 0.1T_c$ ).

$= \sqrt{15/4} \sin^2 \theta \cos 2\phi$ . The form of the gap function is a natural choice for spherical Fermi surface. The question is, can we guess for which field direction in the basal plane ZEDOS is maximum based on the calculation for polar state? Namely, if the magnetic field  $H \perp c$  is along the node, then all QP flowing perpendicular to the field experience zero-energy gap (see inset in Fig. 3) analogous to polar state with  $H \parallel c$ . If the field is along the antinode direction then QP that flow perpendicular to the field experience zero gap only if their momenta are along the  $c$  axis, analogous to polar state and  $H \perp c$ . These simple qualitative arguments, suggesting  $N(E=0, antinode) < N(E=0, node)$ , are misleading since our calculation gives opposite result. It is because one must take into account the contribution from QP that are flowing at some angle with respect to the field in this 3D problem. It is instructive to see how angle-resolved ZEDOS  $N(E=0, \mathbf{v})$ , averaged over angle  $\phi'$  in plane perpendicular to field, changes with angle  $\theta'$  between QP velocity  $\mathbf{v}$  and vortex axis. We plot this quantity, multiplied with weighting factor  $\sin \theta'$  in Fig. 3 at some very low field. Total ZEDOS is area under the curve. Two field directions perpendicular to the  $c$  axis are considered, *node* and *antinode*. For QP that flow perpendicular to the magnetic field,  $\theta' = 90^\circ$ , ZEDOS for node field direction is about three times larger than for antinode field direction. However, for antinode direction QP experience gap node as long as the angle between QP velocity and field direction is  $45^\circ < \theta' < 90^\circ$ . In spite of the  $\sin \theta'$  weighting factor there is a significant contribution to the total ZEDOS that are coming from these QP. As a result, at low field  $N(E=0, antinode)$  is larger than  $N(E=0, node)$  by a few percents.

In Fig. 4(a) field dependence of ZEDOS for node and antinode field directions is shown. Exponent  $\beta \approx 0.32$  for antinode direction differs from  $\beta \approx 0.45$  of polar state ( $H \perp c$ ) in Fig. 1. This difference comes from the different power expansion of the gap function in the node vicinity. In the antinode case, in plane perpendicular to the field, gap function can be approximated as  $|\Omega(\phi, \theta)| \approx \Omega_0 \theta^2$  in the vicinity of gap node  $\theta = 0$ . On the other hand,  $|\Omega(\phi, \theta)| \sim |\theta \pm \pi/2|$  near node  $\theta = \pm \pi/2$  for polar state and  $H \perp c$ . The latter case is analogous to 2D  $d$ -wave function and  $H \parallel c$  giving  $\beta$

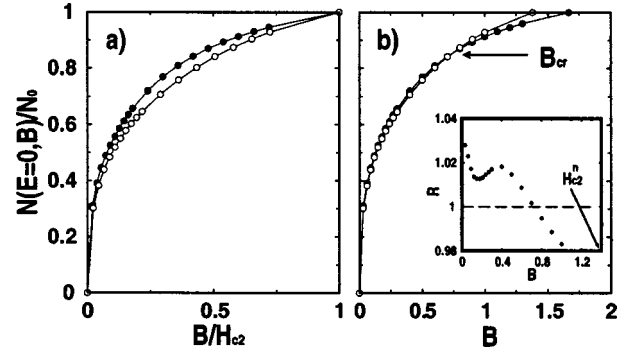


FIG. 4. (a) Field dependence of ZEDOS for antinode (full circles) and node (empty circles) field directions. The best fit to low-field ( $B < 0.25 H_{c2}$ ) dependence is  $N(E=0, B)/N_0 \approx 1.14 \times (B/H_{c2})^{0.324}$  (antinode) and  $N(E=0, B)/N_0 \approx 1.07 \times (B/H_{c2})^{0.327}$  (node). (b) ZEDOS is plotted vs induction  $B$  (in dimensionless units). In the inset ratio  $R = N(antinode)/N(node)$  is shown as a function of induction;  $H_{c2}^n$  denotes upper critical field along node direction.

$\approx 0.45$ . It was shown by Barash and Svidzinsky<sup>10</sup> that temperature dependence of specific heat is closely related to the exponent  $n$  of gap function power expansion near node. The larger is exponent  $n$ , the faster specific heat  $C_s$  is increasing with  $T/T_c$ . Similar qualitative arguments can be applied to field dependence of specific heat.

At  $B = B_{cr}$ , two ZEDOS curves cross, the same as for polar and axial state, see Fig. 4(b). In the inset of Fig. 4(b), ratio  $R = N(antinode)/N(node)$  is plotted against induction  $B$ . Physics of the crossing is very simple and will be explained on the 3D  $d$ -wave case. In the present model, the Fermi surface is assumed to be sphere and upper critical field anisotropy is determined by the gap function. For our simple 3D  $d$ -wave case,  $H_{c2}^{node} < H_{c2}^{antinode}$ . Therefore, for a fixed high field,  $N(E=0, node) > N(E=0, antinode)$  because along the node field direction the superconductor is closer to the normal state and ZEDOS is closer to the normal state value  $N_0$ . On the other hand, for  $B \ll H_{c2}$ , the QP excitations probe the gap structure, since the biggest contribution to the ZEDOS is coming from the delocalized QP. It was calculated  $N(E=0, node) < N(E=0, antinode)$ .

The value of crossing field  $B_{cr}$  depends on the Fermi surface model. Upper critical field is also affected by the Fermi surface anisotropy, and can reverse the sign of four-fold  $H_{c2}$  oscillations in the basal plane. For example, in  $YNi_2B_2C$  the gap node is along  $[100]$ ,  $[010]$  directions, implying that those are also the directions of  $H_{c2}$  minima. But in borocarbides the Fermi surface is highly anisotropic. If we accept that  $LuNi_2B_2C$  has similar electronic structure as Y-borocarbide, then minimum of upper critical field along  $[110]$  direction<sup>11</sup> implies the decisive role of the Fermi surface on  $H_{c2}$  anisotropy. Thus, in this case, the high field inequality should be  $N(E=0, node) < N(E=0, antinode)$ . Since we expect that the Fermi surface anisotropy has no role in low-field ZEDOS, then the sign of fourfold ZEDOS oscillation should be the same for all  $B$ , i.e., there is no crossing of two ZEDOS lines.

In Fig. 5 low-field angular dependence of ZEDOS for

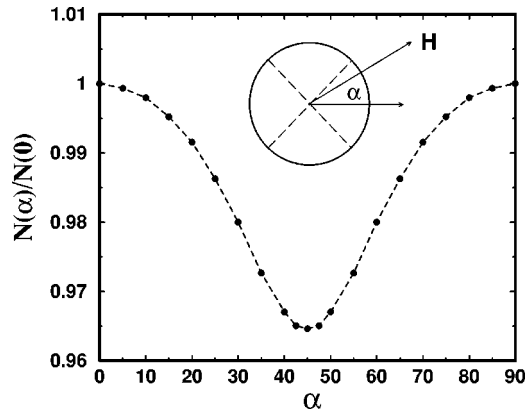


FIG. 5. ZEDOS at  $B=0.0217H_{c2}^{node}$  as a function of angle  $\alpha$  between the applied field and antinode direction.

field rotating in the basal plane is shown. Fourfold oscillation is what one expects from the symmetry of the gap function. Angular variation is  $\approx 3\%$  at low fields, which is measurable with present experimental techniques.<sup>4</sup> Note that in the 2D  $d$ -wave case Doppler-shift calculation<sup>12</sup> estimates angular variation as large as 30%. Parabolalike minimum in angular dependence of ZEDOS is in contrast with cusplike minimum in 2D  $d$ -wave case (and the cylindrical Fermi surface).<sup>12-14</sup>

Cusplike minimum in thermal conductivity angular dependence is predicted in the  $s+g$  model (point node) and observed experimentally.<sup>2</sup> While shape of ZEDOS minimum can rule out some forms of the gap function, it cannot provide the unique answer on the question of node topology (line or point). It is necessary to tilt the field out of the basal plane and study ZEDOS to gain additional information. This was done by measuring thermal conductivity<sup>2</sup> and specific heat<sup>4</sup> with fields rotating around  $c$  axis in  $YNi_2B_2C$ .

We have studied the orientational field dependence of the nodal QP with zero-energy in the mixed state for the three representative gap functions, namely, axial, polar, and  $d_{x^2-y^2}$  states. Our computation is based on quasiclassical approach for the 3D Fermi sphere. We have demonstrated that the orientational dependence and angle-resolved specific heat measurements are ideal tools to distinguish line and point nodes and to locate the nodal direction free from scattering time or localization effects associated with transport experiments and also that this can be feasible in the present day technical limitations. When conducting field-rotation experiment, it is important to keep the field low ( $B < B_{cr}$ ) to probe the intrinsic gap structure.

We thank Y. Matsuda, T. Sakakibara, K. Izawa, I. Vekhter, M. B. Salamon, and T. Park for useful discussions.

<sup>1</sup>M. Sigrist and K. Ueda, Rev. Mod. Phys. **63**, 239 (1991); K. Machida, Prog. Theor. Phys. Suppl. **108**, 229 (1992).

<sup>2</sup>K. Izawa *et al.*, Phys. Rev. Lett. **89**, 137006 (2002), and earlier references therein.

<sup>3</sup>See, for example, F. Yu *et al.*, Phys. Rev. Lett. **74**, 5136 (1995). Here angle-dependent  $\kappa$  shows maximum at the nodal direction for  $d_{x^2-y^2}$ -cuprate, which is opposite to that expected by QP contribution. Also see an interesting argument between  $\kappa(H)$  and  $\gamma(H)$ . E. Boaknin *et al.*, *ibid.* **90**, 117003 (2003).

<sup>4</sup>T. Park *et al.*, Phys. Rev. Lett. **90**, 177001 (2003).

<sup>5</sup>T. Dahm *et al.*, Phys. Rev. B **66**, 144515 (2002).

<sup>6</sup>M. Ichioka *et al.*, Phys. Rev. B **59**, 184 (1999).

<sup>7</sup>P. Miranović and K. Machida (unpublished).

<sup>8</sup>N. Nakai, M. Ichioka, and K. Machida, J. Phys. Soc. Jpn. **71**, 23 (2002).

<sup>9</sup>V.P. Mineev and K.V. Samokhin, *Introduction to Unconventional Superconductivity* (Gordon and Breach, The Netherlands, 1999), p. 102.

<sup>10</sup>Yu.S. Barash and A.A. Svidzinsky, Phys. Rev. B **53**, 15 254 (1996).

<sup>11</sup>V. Metlushko *et al.*, Phys. Rev. Lett. **79**, 1738 (1997).

<sup>12</sup>I. Vekhter *et al.*, Phys. Rev. B **59**, R9023 (1999).

<sup>13</sup>P.J. Hirschfeld, J. Korean Phys. Soc. **33**, 485 (1998).

<sup>14</sup>E. Schachinger and J.P. Carbotte, Phys. Rev. B **60**, 12 400 (1999).